Colloquium

Quantum effects in dynamics of water and other liquids of light molecules

V.N. Novikov[1,2,3,a] and A.P. Sokolov[1,2,4,5]

[1] Department of Chemistry, University of Tennessee, Knoxville, TN 37996, USA
[2] Shull Wollan Center – Joint-Institute for Neutron Sciences, Oak Ridge National Laboratory and University of Tennessee, Oak Ridge, TN 37831, USA
[3] Institute of Automation and Electrometry, Russian Academy of Sciences, Novosibirsk, 630090, Russia
[4] Chemical Sciences Division, Oak Ridge National Laboratory, Oak Ridge, TN 37831, USA
[5] Department of Physics and Astronomy, University of Tennessee, Knoxville, TN 37996, USA

Abstract. Nuclear quantum effects in atomic motions are well known at low temperatures $T < 10$ K, but analyses of structural relaxation in liquids and description of the glass transition traditionally neglect quantum effects at higher temperatures, $T > 50$–100 K. Recent studies, however, suggested that nuclear quantum effects in systems of light molecules (*e.g.*, water) might play an important role in structural dynamics and provide non-negligible contributions at such temperatures, and even up to ambient temperature. In this article, we discuss experimental evidences of the quantum effects in glass transition in liquids of light molecules and possible theoretical descriptions of these effects. We show that quantum effects may qualitatively change the temperature behavior of the structural relaxation time in supercooled liquids leading to deviations of some well-established properties of the glass transition when it happens at low temperatures. We also demonstrate that unusual behavior of water dynamics at low temperatures, including apparent fragile-to-strong crossover, can be ascribed to nuclear quantum effects.

1 Introduction

Quantum effects in structural dynamics of condensed matter are well known at very low temperatures, usually below ~ 10 K [1–7]. They include atomic tunneling, zero-point vibrations and associated energy, and indistinguishability of particles. Traditional examples are two-level systems in amorphous solids that manifest themselves in specific heat, damping of acoustic modes [1–5], rotation of methyl groups [6], several chemical reactions [7]. The contribution of these quantum effects to structural relaxation usually is neglected at temperatures above ~ 20–50 K. However, it is becoming increasingly evident that quantum effects in structural dynamics may be essential at much higher temperatures, 100–200 K. For example, it has been known for some time that quantum effects can play a role in the melting of small clusters [8]. Recent simulations of Lennard-Jones systems [9,10] and also quantum generalization of the mode-coupling theory of the glass transition [11] suggest that zero-point vibrations and tunneling might play an essential role in the dynamics of glass-forming liquids, and can either slowdown or accelerate the dynamics. Simulations also suggested that quantum effects might be es-

sential in the diffusion of water molecules even at ambient temperature [12–14]. Recently, the influence of the quantum effect on the glide of dislocations was found at unusually high temperatures [15]. The authors have shown that zero-point vibrations ease dislocation motions at temperatures up to ~ 60 K.

In many traditional well-studied cases (*e.g.*, two-level systems in glasses, methyl group rotation) quantum effects in dynamics have been analyzed in the picosecond-microsecond time range [6,7]. Since the structural relaxation at glass transition takes much longer time on the order of seconds-minutes, even low-probability tunneling rate may become comparable with that of the thermal activation at relatively high temperatures, especially for light molecules. These results raise several fundamental questions: Can quantum effects be important in the structural dynamics of supercooled liquids of light molecules? Or liquids will solidify long before any quantum effects have significant impact on structural relaxation? How low should be the glass transition temperature for quantum effects to be important and how will they affect the glass transition? Which materials can show non-negligible quantum effects in the glass transition?

These are the types of questions we are discussing in this short review. First, we briefly present a theoretical

a e-mail: novikov@utk.edu

basis of quantum effects, such as tunneling and zero-point vibrations and energy, in the glass transition in sect. 2. Some predictions for the influence of the quantum effects on the temperature dependence of structural relaxation and on the glass transition temperature of supercooled liquids are discussed in sect. 3. The presented analysis emphasizes the critical importance of the molecular mass for quantum effects. One of the lightest molecules is water, and the role of quantum effects in the water's glass transition is the major focus of our discussion in sect. 4. To discuss the dynamics of supercooled water in a broader temperature range we turn to the analysis of the dynamics of confined water in sect. 5. In the end, we discuss the possibility of quantum effects in the structural dynamics of other light molecule liquids and emphasize that neglecting quantum effects in simulations might be one of the major reason for their failure to reproduce consistently the properties of water.

2 Theoretical basis

The relative importance of the quantum effects at a temperature T is usually quantified by the dimensionless parameter $\Lambda^*(T)$, which is the ratio of a particle thermal de Broglie wavelength to the interatomic distance a,

$$\Lambda^* = \frac{\hbar}{a\sqrt{k_B M T}}. \tag{1}$$

As the thermal wavelength increases, Λ^* increases and the significance of quantum behavior also increases. Λ^* is related to the de Boer parameter $\Lambda = \hbar/(a\sqrt{k_B M \epsilon})$ [16] as $\Lambda^* = (\epsilon/k_B T)^{1/2}\Lambda$ where ϵ is the well depth of the pair potential [17]. Λ is useful for comparing the degree of the quantum character of different liquids at a given temperature. How large should be Λ^* (*i.e.*, how low should be temperature and/or mass of the particles) in order for quantum effects in the glass transition to be comparable to the thermal ones is not clear *a priori*.

In order to understand how large should be the quantum parameter Λ^* to make quantum effects in the glass transition comparable to classical thermal effects, we perform a rough estimation of the nuclear tunneling rate at T_g, and compare it with the classical thermal activation rate. Usually, the structural α-relaxation process in supercooled liquids is described as a thermally activated jump over a potential energy barrier. The probability of the jump is

$$W = \tau_\alpha^{-1}(T) = \tau_0^{-1}\exp\left(-\frac{E_a(T)}{k_B T}\right). \tag{2}$$

Here $\tau_0^{-1} \propto M^{-1/2}$ is an attempt frequency, $E_a(T)$ is the activation energy. In general, there is a finite probability for a particle to tunnel under the barrier. At very low temperatures, activation processes become negligible and quantum tunneling might dominate the structural relaxation. For a rough estimate of the tunneling rate we use the quasi-classical approximation for the tunneling of a

particle with the energy E given by the Wentzel-Kramers-Brillouin (WKB) equation [18]:

$$\tau_\alpha^{-1}(T) = \tau_0^{-1}\exp[-A_{tun}(E)], \tag{3}$$

$$A_{tun}(E) = \frac{2}{\hbar}\int_{x_1}^{x_2}[2M(U(x) - E)]^{1/2}\mathrm{d}x. \tag{4}$$

Here $U(x)$ is the potential barrier, and $E < U(x)$ for x between x_1 and x_2. As has been shown in ref. [19], A_{tun} at low T is of the order of E_b/E_0 for any reasonable potential, where E_b is the height of the potential barrier and $E_0 = \hbar\omega/2$ is the zero-point energy.

Thus, in general, the role of quantum effects increases drastically with an increase of zero-point energy relative to the characteristic energy barrier controlling the structural relaxation. At the glass transition temperature, by definition, $\ln\tau_\alpha(T_g)/\tau_0 \sim \ln 10^{17} \sim 39$. It means that the tunneling rate becomes comparable to the thermally activation rate at T_g if $E_b/E_0 \leq 39$. In the case of a purely thermally activated structural relaxation one has $E_b/T_g \sim 39$, so $E_b \sim 39T_g$. This leads to the condition $T_g/E_0 < 1$ for quantum effects to be important at T_g. In terms of vibrational frequency, $T_g/\hbar\omega < 1/2$. Taking as a characteristic vibrational frequency the Debye frequency, this condition can be represented as

$$T_g/\theta_D < 1/2, \tag{5}$$

where θ_D is the Debye temperature. We will see below that a similar result can be obtained in other approaches.

Returning to the quantum de Boer parameter (1), it can be shown that in the Debye model of vibrations one can express Ma^2 in eq. (1) through T_g and θ_D using the Lindemann criterion of melting. As a result, $\Lambda^* = \frac{\gamma}{3}\frac{\theta_D}{\sqrt{T_g T}}$, where $\gamma = (r^2(T_g)/a^2)^{1/2} \approx 0.12$–$0.15$ is the Lindemann parameter [20]. In particular, at the glass transition

$$\Lambda^*(T_g) = (\gamma/3)\theta_D/T_g \approx 0.05\theta_D/T_g. \tag{6}$$

Thus, the condition (5) roughly corresponds to $\Lambda^*(T_g) > 0.1$. This estimate agrees with the simulation data (fig. 2(a) in ref. [9]) that predicted the onset of quantum effects for diffusion in a supercooled liquid in this range of Λ^*. The interpretation of this crossover value of $\Lambda^*(T_g)$ can be connected to the Lindemann criterion of melting. The tunneling contribution to the structural relaxation is comparable to the thermal one at T_g if the thermal wavelength $\hbar\sqrt{k_B M T_g}$ is equal to or larger than $\sim 0.1a$, the latter value corresponds to the amplitude of atomic vibrational displacements at T_g according to the Lindemann criterion of melting [20].

Having this estimate, one can better understand the range of temperature and molecular mass at which quantum effects may be essential at the glass transition. Figure 1 shows the dependence of Λ^* on the molecular mass in several molecular liquids at $T = 2T_m/3$, T_m is the melting temperature. The chosen temperature $(2/3)T_m$ is assumed to be close to T_g [21]. Actual T_g in low-temperature liquids might be smaller than $2T_m/3$ [22] and, respectively,
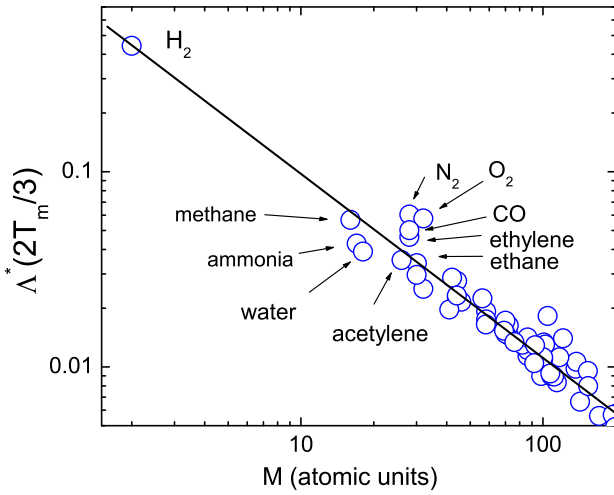
Fig. 1. The dependence of the parameter $\Lambda^*(T)$ on the molecular mass in molecular liquids at $T = 2T_m/3$ (expected glass transition temperature). The length a was estimated as $(M/\rho)^{1/3}$ where M is the molecular mass and ρ is the density in the liquid state.

$\Lambda^*(2T_m/3) \geq \Lambda^*(T_g)$. One can see that Λ^* is significantly larger than 0.1 for hydrogen, and there are some molecular liquids, such as methane, ammonia and water, where Λ^* is close to 0.1.

Using the definition of $\Lambda^*(T_g)$ (eq. (1)) the condition $\Lambda^*(T_g) > 0.1$ corresponds to

$$a^{*2}NT < 5000, \qquad (7)$$

where a^* is the average intermolecular distance in angstroms, and $N = M/M_0$ is the molecular mass in atomic units ($M_0 = 1.66 \times 10^{-24}$ g). For example, if $a^* \sim 1.5$ Å, then $T\,(\mathrm{K}) < 2200/N$. So, such materials as water ($N = 18$) or methane ($N = 16$) may have essential quantum effects in the structural relaxation even at $T > 100$ K. Of course, these estimates have accuracy only by the order of magnitude.

To provide more quantitative analysis of the role of the quantum effects, we will consider two approaches: The first one is microscopic that takes into account the specific parameters of the interparticle potential. The second one is phenomenological in nature and is based on the elastic theory of the glass transition [23,24].

2.1 Direct account of tunneling in a double-well potential

Let us consider the probability of the over-barrier relaxation and tunneling in the double-well potential (fig. 2) in more details, although still in a very simplified form. A particle can escape a potential well either by a thermally activated jump or by tunneling through the barrier. In this approach the total rate of the relaxation is found as a sum of the contribution from the thermally activated jumps and from the tunneling under the barrier in the same potential [25]. The potential is a harmonic one,
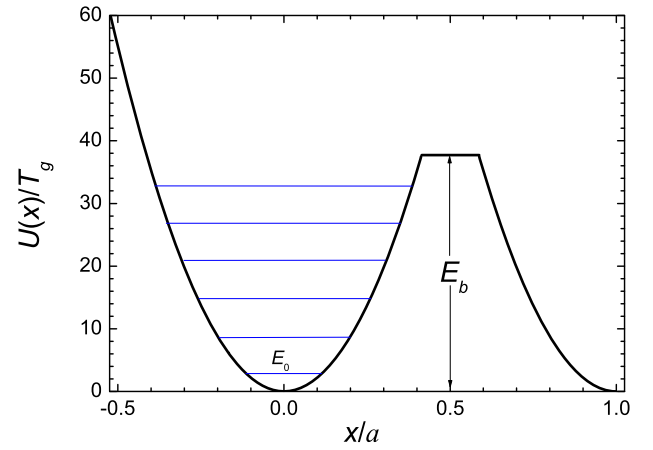
Fig. 2. Schematic representation of the potential well used to estimate the tunneling probability. Blue lines correspond to different quantum levels.

$U(x) = kx^2/2$, $k = M\omega^2$, till the top, where it acquires a constant value E_b (fig. 2). The tunneling can go from each of the quantum levels with the energy E_n, so the total rate $\tau_\alpha(T)$ for the particle to escape the well can be written as

$$\tau_\alpha^{-1}(T) = \tau_0^{-1} P(E > E_b, T) + \sum_n \Gamma(E_n, T) P(E_n, T). \qquad (8)$$

The first term in the rhs of eq. (8) describes the thermally activated jumps over the barrier with the height E_b, and $P(E > E_b, T)$ is the probability for a particle in the well to have the energy $E > E_b$. The second term describes the probability of tunneling from all energy levels with energies $E_n < E_b$. $P(E_n, T)$ is the probability to occupy the level with the energy E_n, and $\Gamma(E_n, T)$ is the tunneling rate, which on the time scale of the glass transition can be estimated in the WKB approximation as

$$\Gamma(E_n, T) = \tau_0^{-1} \exp\left[-\frac{2}{\hbar} \int_{x_1}^{x_2} \sqrt{2M(U(x) - E_n)}\,\mathrm{d}x\right]. \qquad (9)$$

The potential $U(x)$ is fixed by the curvature at the bottom of the well (connected to the elastic constant k), the barrier height E_b, and the barrier half-width at the bottom $a/2$.

The probability $P(E_n, T)$ is equal to

$$P(E_n, T) = A_1 \exp(-E_n/T), \qquad (10)$$

where the constant A_1 is determined by the normalization condition

$$\sum_{n=0}^{\infty} P(E_n, T) = 1. \qquad (11)$$

For the harmonic potential $E_n = \hbar\omega(n + 1/2)$, so the constant A_1 can be found from the equation

$$A_1\left(e^{-\frac{\hbar\omega}{2T}} \sum_{n=0}^{n_{max}} e^{-\frac{\hbar\omega n}{T}} + \int_{E_b/T}^{\infty} e^{-x}\mathrm{d}x\right) = 1 \qquad (12)$$

where n_{max} is the integer part of $(E_b/\hbar\omega - 1/2)$.

As a result,

$$A_1 = \left(e^{-\frac{\hbar\omega}{2T}} \frac{1 - \exp(-\frac{\hbar\omega(n_{max}+1)}{T})}{1 - \exp(-\frac{\hbar\omega}{T})} + e^{-\frac{E_b}{T}} \right)^{-1}. \quad (13)$$

Usually $\exp(E_b/T) \gg 1$, so one can rewrite eq. (13) as

$$A_1 \approx e^{\frac{\hbar\omega}{2T}}. \quad (14)$$

We note that $\hbar\omega/2$ in eq. (14) is the zero-point energy E_0. The expression for the escape rate is now

$$\tau_\alpha^{-1}(T) = \tau_0^{-1} e^{-\frac{E_b - E_0}{T}} + \tau_0^{-1}$$
$$\times \sum_{n=0}^{n_{max}} e^{-\frac{E_n - E_0}{T} - \frac{4\sqrt{2M}}{\hbar} \int_{x_{1n}}^{x_{2n}} \sqrt{\frac{kx^2}{2} - E_n} dx}. \quad (15)$$

The limits of the integral in eq. (15) are equal to $x_{1n} = (2E_n/k)^{1/2}$, $x_{2n} = a/2$. Denoting

$$z_n = \frac{x_{1n}}{a} = \sqrt{\frac{2E_n}{ka^2}} \quad (16)$$

and explicitly taking the integral in eq. (15) we have

$$\tau_\alpha^{-1}(T) = \tau_0^{-1} \exp\left(-\frac{E_b - E_0}{T}\right) + \tau_0^{-1} \sum_{n=0}^{n_{max}} \exp\left\{ -\frac{E_n - E_0}{T} \right.$$
$$\left. -\frac{a\sqrt{kM}}{\hbar} \left[2\sqrt{1 - z_n}\,(2 - z_n) + z_n^2 \ln \frac{z_n}{2 + 2\sqrt{1 - z_n} - z_n} \right] \right\}. \quad (17)$$

This equation will be used later in sect. 4 to analyze the temperature dependence of the structural relaxation time in deeply supercooled water. Although it is only schematic, it catches the essential parameters of the problem and can be compared with the experimental data. As we will show below, this estimate predicts that the tunneling is essential at T_g in water, with reasonable values of the parameters of the effective potential.

2.2 Accounting for quantum effects in the elastic theory of the glass transition

The characteristic conditions needed for the importance of the quantum effects in the structural relaxation can be evaluated using a more phenomenological approach. According to the elastic theory of the glass transition [23, 24], the structural relaxation time is equal to

$$\tau_\alpha(T) = \tau_0 \exp\left(\frac{A}{r^2}\right), \quad (18)$$

where r^2 is the mean-square particle displacement (MSD), $A = \lambda_1 a^2$ and λ_1 is a constant of the order of one. This equation was first derived in ref. [26]. It was used for the description of the structural relaxation in many other papers [27–30]. The expression (18) was later improved

by suggesting non-linear relationships between $\log \tau_\alpha$ and $1/r^2(T)$ [31–33], which provided a better agreement with experimental data. In ref. [31] the spatial fluctuations of the parameter A in eq. (18) are taken into account, which leads to a universal expression for τ_α:

$$\log \tau_\alpha = a_0 + a_1 r^2(T_g)/r^2(T) + a_2(r^2(T_g)/r^2(T))^2, \quad (19)$$

with $a_0 = -11.922$, $a_1 = 1.622$, and $a_2 = 12.3$ (assuming $\log \tau_\alpha(T_g) = 2$).

Based on some analogy to the free-volume model, a power law relationship was proposed in [32, 33]:

$$\tau_\alpha = \tau_0 \exp[A/r^2(T)]^{\alpha/2} \quad (20)$$

with the exponent $\alpha \sim 3$.

The expressions (18)–(20) were derived in the classical thermally activated regime of structural relaxation, thus they assumed only the thermal contribution to MSD. However, total MSD includes the contribution of zero-point oscillations, which are essential at low T:

$$r^2 = r_T^2 + r_0^2, \quad (21)$$

here r_T^2 corresponds to thermal fluctuations, and r_0^2 to quantum fluctuations. It is not obvious *a priori* whether the elastic theory of the glass transition should use the total MSD, including zero-point vibrations. We will show below that including zero-point MSD into eqs. (18)–(20) can be justified as a good zeroth-order approximation that takes into account tunneling effects in structural relaxation.

The total vibrational MSD can be expressed via the vibrational density of states $g(\omega)$ as [34]

$$r^2(T) = \frac{1}{M} \int \frac{g(\omega)}{\omega} \left(n(\omega, T) + 1/2 \right) d\omega. \quad (22)$$

Here $n(\omega, T) = (\exp(\hbar\omega/k_B T) - 1)^{-1}$ is the temperature-dependent Bose factor.

Respectively,

$$r_T^2(T) = \frac{1}{M} \int \frac{g(\omega)}{\omega} n(\omega, T) d\omega \quad (23)$$
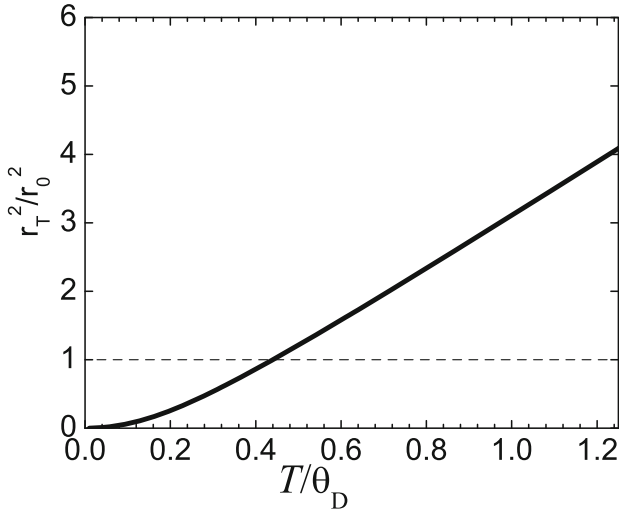
and

$$r_0^2 = \frac{1}{2M} \int \frac{g(\omega)}{\omega} d\omega. \quad (24)$$

In the Debye model of vibrations $g(\omega) = 9\omega^2/\omega_D^3$, where $\omega_D = c_D(6\pi^2 n)^{1/3}$ is the Debye frequency, n is the particle number density, $c_D = (3/(c_l^{-3} + 2c_t^{-3}))^{1/3}$ is the Debye sound velocity, and c_l and c_t are the longitudinal and transversal sound velocities, respectively. With this density of states

$$r_T^2 \approx \frac{9k_B T}{M\omega_D^2} \quad \text{at } T \geq \hbar\omega_D \quad (25)$$

and

$$r_0^2 \approx \frac{9\hbar}{4M\omega_D}. \quad (26)$$

Fig. 3. The ratio of the thermal MSD r_T^2 to the zero-point MSD r_0^2 in the Debye model of vibrations. The dashed horizontal line corresponds to $r_T^2 = r_0^2$.

From eqs. (5) and (26) it follows that $M\omega_0 = 9/(4r_0^2)$, thus $A_{tun} \sim \lambda_2 a^2/r_0^2$, where $\lambda_2 \sim 2E_b/M\omega_0^2 a^2$ is a constant of the order of one. A similar expression is derived for A_{ther} [23,24]: $A_{ther}(T) \sim \lambda_1 a^2/r_T^2$.

To combine two limiting regimes, one dominated by the over-barrier relaxation A_{ther}, and another by the tunneling A_{tun}, one could employ the simplest Padé-like approximation for $\log \tau_\alpha$, and the exponent $A(T)$ at all temperatures can be represented roughly as

$$1/A = 1/A_{ther} + 1/A_{tun}. \qquad (27)$$

This approximation correctly reproduces the expected low-temperature quantum limit ($A_{ther} \to 0$, $A = A_{tun}$) and high-T limit ($A_{ther}(T) \ll A_{tun}$, $A = A_{ther}(T)$). Based on these two limits, it also makes a simple extrapolation into the intermediate region where both amplitudes are comparable.

From eq. (27) we have

$$A = \frac{\lambda_1 a^2}{r_T^2 + \beta r_0^2} , \qquad (28)$$

where $\beta = \lambda_1/\lambda_2$ is a constant of the order of one. Thus, by considering r^2 in eq. (18) as the total MSD that includes zero-point vibrations, we roughly take into account the tunneling effect. It becomes comparable with the thermal relaxation when $r_T^2 \sim r_0^2$. The analysis of the ratio r_T^2/r_0^2 in the Debye model of vibrations (fig. 3) suggests that thermal and zero-point contributions to the total MSD become comparable at $T/\theta_D \sim 0.5$. It means that a significant influence of quantum effects on the glass transition might be expected if $T_g/\theta_D < 0.5$, in agreement with eq. (5) obtained by a different method. We note that this estimate in the Debye model does not take into account a possible non-linear (anharmonic) temperature dependence of r_T^2. However, in most cases it should not be too important at temperatures below or close to T_g where anharmonic

contributions to MSD are small enough to be neglected in the present estimate. For example, for water, the anharmonic contribution to MSD at T_g is less than 10% [25], as we will discuss in more detail below. Another factor that influences the relation between r_T^2 and r_0^2 is the excess (in comparison with the Debye model) of low-frequency vibrational modes, *i.e.* the boson peak [22]. These vibrations enhance thermal MSD in comparison with the quantum fluctuations, so the condition $r_T^2 = r_0^2$ shifts to lower temperature in comparison with the prediction of the Debye model. The shift might be 10–20% depending on the strength of the boson peak [22].

3 Influence of quantum effects on glass transition temperature and fragility

3.1 Shift of T_g

The tunneling adds an additional channel of structural relaxation that competes with the usual thermally activated relaxation. This should lead to a decrease of the glass transition temperature in comparison with the one expected in the case without tunneling. It was proposed in [22] that such a shift may be detected by comparison of T_g and the melting temperature T_m. It is well known from the analysis of experimental data that for most of glass-formers the ratio T_g/T_m is about 2/3 [21]. Since T_m is $\sim 1.5 * T_g$, the influence of quantum effects on T_m should be much smaller than on T_g. Thus, the shift of T_g to lower temperatures due to quantum effects should be stronger than that of T_m and should decrease the ratio T_g/T_m from its classical value $\sim 2/3$.

To estimate the shift of T_g, the Lindemann-like argument is used [22]. Assuming that in the classical case the glass transition temperature would be T_{g0} and the quantum fluctuations shift it to T_g one can write the relation between T_{g0} and T_g as $r_0^2 + r_T^2(T_g) = r_T^2(T_{g0})$. In harmonic approximation MSD changes linearly with temperature, and at T_g it can be represented as $r_T^2(T_{g0}) = bT_{g0}$, and $r_T^2(T_g) = bT_g$ where the factor b is determined by the elastic properties of the glass. Thus, in this approximation the shift of the glass transition temperature is described by the relation

$$r_0^2 + bT_g = bT_{g0}. \qquad (29)$$

Assuming the usual classical relation between T_{g0} and T_m, $T_{g0} \sim CT_m$, where $C \approx 2/3$, eq. (29) can be rewritten as $r_0^2/b + T_g = AT_m$. In the Debye model of vibrations $r_0^2/b = \theta_D/4$ as it follows from eq. (25). This leads to a simple relationship between T_g and T_m of the system:

$$\frac{T_g}{T_m} = \frac{A}{1 + \frac{r_0^2}{bT_g}} \approx \frac{A}{1 + \frac{\theta_D}{4T_g}} . \qquad (30)$$

Equation (30) predicts that quantum effects should lead to a significant decrease of the ratio T_g/T_m with decreasing T_g/θ_D.

Using eq. (30) one can find the dependence of the ratio T_g/T_m on T_g if one knows how θ_D scales with T_g. In

ref. [22] it was noted that in various materials θ_D variates much weaker than T_g, so for fitting purposes in a rough approximation it was taken a constant. Here we are taking into account variations of both T_g and θ_D. In harmonic approximation, the relation between ω_D and T_g is

$$M\omega_D^2 r_g^2 \sim k_B T_g. \tag{31}$$

The Lindemann criterion applied at T_g gives $u_g^2 = \gamma^2 a^2$ where a is a characteristic intermolecular distance, $a \propto V_m^{1/3}$, V_m is the molecular volume, M is the molecular mass and $\gamma \sim 0.12$–0.13 is a universal Lindemann constant. As a result,

$$\omega_D \sim \left(\frac{k_B T_g}{M}\right)^{\frac{1}{2}} \frac{1}{\gamma a}. \tag{32}$$

At this point we apply the scaling relation between the molecular mass and T_g in molecular glass-formers that was found in ref. [35]: $T_g \propto M^p$, where the exponent $p \sim 1/2$. Assuming also some average density for molecular glass-formers one can find that $a \propto V_m^{1/3} \propto M^{1/3} \propto T_g^{2/3}$. As a result, eq. (32) gives the following dependence of the T_g/T_m ratio on T_g:

$$\frac{T_g}{T_m} = \frac{D}{1 + (T_0/T_g)^{13/6}}. \tag{33}$$

In eq. (33) D and T_0 are just constants, $T_0 = (\hbar/4\gamma k_B^{1/2})^{6/13}(4\pi\rho/3)^{2/13}(T_1^2/M_0)^{5/13}$, where ρ is the average density, M_0 is the atomic mass unit and $T_1 = 14.4$ is a coefficient in the correlation $T_g = T_1(M/M_0)^{1/2}$ [35]. Equation (33) shows that at high T_g, $T_g/T_m \sim D$. However, the ratio T_g/T_m decreases strongly with decrease in T_g.

The analysis of the literature data in molecular and hydrogen-bonding glass-formers indeed reveals the predicted strong decrease in the T_g/T_m ratio for materials with T_g below ~ 60–$80\,\mathrm{K}$ (fig. 4). In materials with T_g above $\sim 100\,\mathrm{K}$, the T_g/T_m ratio retains the classical value in the range ~ 0.5–0.8, but it drops to much lower values for materials with T_g below $50\,\mathrm{K}$ (fig. 4). Moreover, eq. (33) provides a reasonable qualitative description for the behavior of T_g/T_m (fig. 4) with the best-fit parameters $D \approx 0.72 \pm 0.01$ and $T_0 \approx 51 \pm 3\,\mathrm{K}$. The constant T_0 can be estimated if one takes $T_1 = 14.4\,\mathrm{K}$ from ref. [35] and also some characteristic density for molecular glass-formers, $e.g.$, $\rho = 1.5\,\mathrm{g/cm^3}$. With these values of parameters one gets $T_0 = 65\,\mathrm{K}$. Although it is larger than one found by the fit, it is a reasonable agreement taking into account the crude level of the estimate and the arbitrary value of density used in the estimation.

These experimental results (fig. 4) suggest that quantum effects can indeed play a significant role in reducing the glass transition temperature in low-T_g materials. A larger relative contribution of the zero-point vibrations at lower temperatures leads to a broadening of the glass transition range by significantly decreasing T_g.
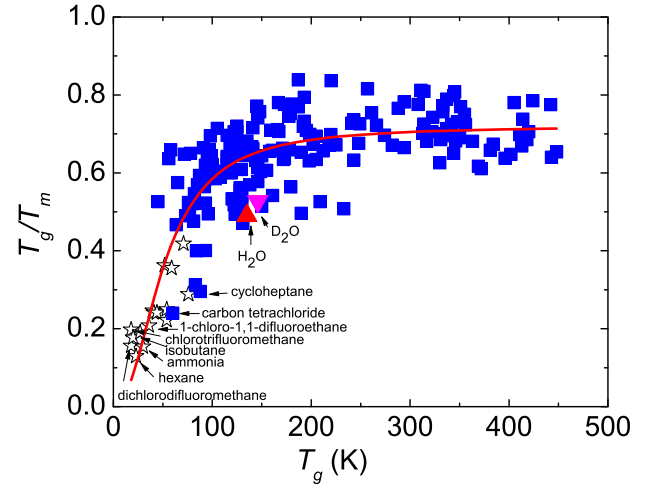
Fig. 4. The dependence of the ratio T_g/T_m on T_g in molecular and hydrogen-bonding glass-formers. The up triangle presents H_2O; the down triangle D_2O (data from ref. [36]). The line is the fit by the expression (14). Stars correspond to estimates of T_g in low-T_g glass-formers from ref. [37]; squares show data from ref. [22].

3.2 Influence of quantum effects on temperature variations of structural relaxation

One of the important characteristics of the glass transition is the steepness of the temperature dependence of the structural relaxation time $\tau_\alpha(T)$ close to T_g. It can be characterized by the so-called fragility index, or steepness index m defined as [38,39]:

$$m = \frac{\partial \log\lceil\tau_\alpha(T)\rceil}{\partial[\frac{T_g}{T}]}\bigg|_{T=T_g}. \tag{34}$$

The least-fragile–known glass-forming systems, covalent bonded silica and BeF_2, exhibit an Arrhenius-like temperature dependence of their viscosity or $\tau_\alpha(T)$ over a broad temperature range above T_g leading to a fragility value of $m \sim 20$–22 [40,41]. Fragility increases strongly in molecular liquids, reaching $m \sim 80$–100 in many van der Waals and ionic liquids [40,41].

It is obvious that a weaker temperature dependence of tunneling should lead to less steep $\tau_\alpha(T)$. In ref. [22] it was shown that the influence of quantum effects on the temperature dependence of τ_α can be described by the inclusion of zero-point MSD to the usual expression of the elastic theory of glass transition, eqs. (18), (21). At sufficiently low T the thermal part becomes smaller than u_0^2. At such temperatures the rate of tunneling is comparable to or larger than the rate of thermally activated transitions. If this happens in the supercooled state, $T \geq T_g$, the temperature dependence of τ_α will be unusually weak, the apparent activation energy will be decreasing with decreasing temperature and fragility will be unusually low [22,42]. To quantify the influence of the quantum effects on fragility m, we use eq. (18) and the definition of m in eq. (34). A
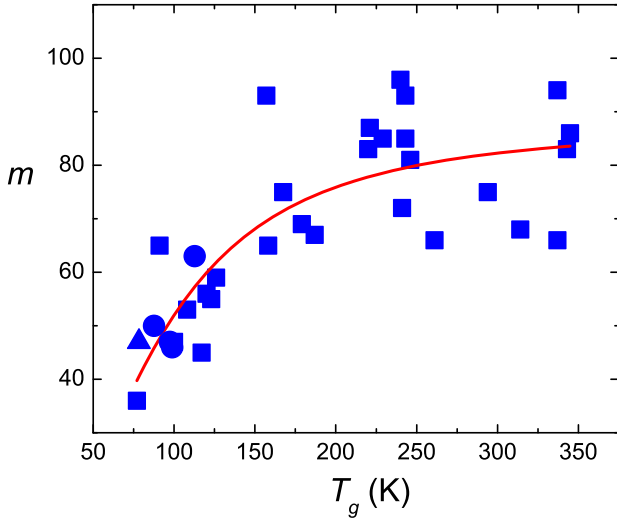
Fig. 5. The dependence of fragility on T_g for molecular liquids. Solid line: fit by eq. (38) with $T_0 = 84$ K. Squares: data from ref. [41]; triangle: 3-MP data from ref. [43]; circles: data from ref. [44].

Fig. 6. Log τ_α estimated according to the universal eq. (19) [31] in the Debye model for various T_g/θ_D ratios. A decrease in the T_g/θ_D ratio leads to a significant decrease in the fragility m (shown in the order corresponding to the curves).

simple estimation gives

$$m = \frac{m_{mol}}{1 + r_0^2/r_g^2}, \qquad (35)$$

where

$$m_{mol} = m_0 \frac{T_g}{r^2(T)} \frac{\mathrm{d}r^2(T)}{\mathrm{d}T}\bigg|_{T=T_g} \qquad (36)$$
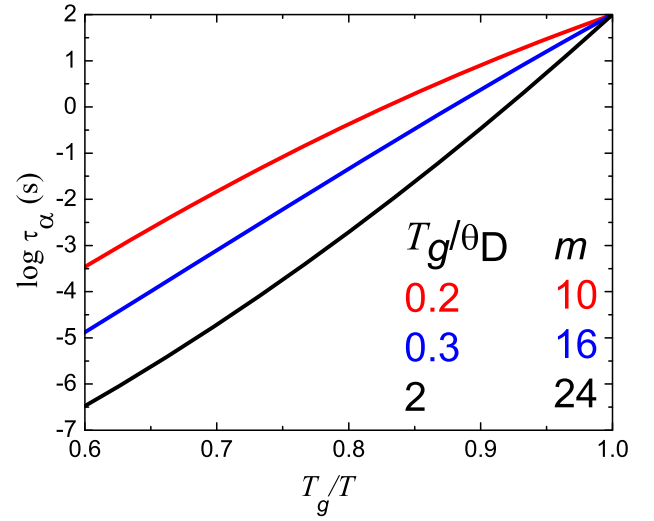
is the fragility of classical molecular supercooled liquids, $m_{mol} \sim 70\text{--}90$, and $m_0 = \log_{10} \tau_\alpha(T_g)/\tau_0$ in the case (eq. (18)), $m_0 = a_1 + 2a_2 = 14.3$ in the case (eq. (19)), and $m_0 = (\alpha/2) \log_{10} \tau_\alpha(T_g)/\tau_0$ in the case (eq. (20)). Thus, eq. (35) follows from the all three versions of the elastic theory of the glass transition, eqs. (18)–(20), with possibly slightly different values of m_{mol}. Taking $r_T^2(T_g)$ and r_0^2 from the Debye model of acoustic vibrations (eqs. (25) and (26)), eq. (36) can be rewritten as

$$m = \frac{m_{mol}}{1 + \theta_D/4T_g}. \qquad (37)$$

This equation is very similar to eq. (33). The analysis of the ratio θ_D/T_g that follows eq. (33) can be applied in exactly the same form here leading to the following dependence of fragility on T_g:

$$m = \frac{m_{mol}}{1 + (T_0/T_g)^{13/6}}. \qquad (38)$$

Equation (38) shows that at high T_g, $m \sim m_{mol} \sim 70\text{--}90$. However, at decreasing T_g, m also decreases due to quantum effects. In fig. 5, the dependence of the fragility on T_g for various molecular glass-formers is shown. We see that at higher temperatures m is more or less T_g-independent and scatters mostly in the range 70–90. However at lower temperatures, $T \leq 100\text{--}120$ K, fragility systematically decreases and drops below $m \sim 50$ in liquids

with $T_g \leq 100\text{--}120$ K. The best fit of the data to eq. (38) gives $m_{mol} = 87 \pm 4$, $T_0 = 84 \pm 8$ K (fig. 5). Although the parameter T_0 differs from the value estimated using T_g (fig. 4), the difference is not very large taking into account the rough approximation used. Thus, the unusually low fragility in low-temperature molecular liquids, such as 2-methyl pentane, might be a signature of moderate quantum effects [42]. We note that although the contribution of anharmonicity to the amplitude of MSD at $T \leq T_g$ in most cases is not significant, the slope of the MSD dependence on T may increase significantly at T_g, especially in fragile systems. We took care of this in our estimate of fragility in eqs. (35)–(37) by using the experimental values of fragility of molecular glass-formers in eq. (36).

A qualitative estimate of the influence of quantum effects on the temperature dependence of τ_α was done in ref. [22] in the framework of the elastic model of the glass transition modified by including zero-point MSD that accounts for tunneling. As was discussed in sect. 2, the importance of quantum effects can be tuned by the ratio of T_g/θ_D. Assuming the Debye model for $r^2(T)$, the temperature dependence of $\tau_\alpha(T)$ can be estimated using eq. (19) with zero-point MSD included (fig. 6). At relatively high T_g ($T_g/\theta_D = 2$), when quantum effects are negligible, eq. (19) predicts a normal behavior for $\log \tau_\alpha$ vs. $1/T$, i.e. a monotonic increase of the slope (apparent activation energy) upon cooling. However, an unusual behavior is predicted for low-T_g materials: one can observe a clear decrease in the apparent activation energy upon approaching T_g when the ratio T_g/θ_D is approximately 0.2–0.3 (fig. 6). For the cases with $T_g/\theta_D = 0.2$ and 0.3, eq. (19) predicts a drop in the fragility index to unusually low values $m \sim 10$ and ~ 16, respectively (fig. 6). We emphasize that the shape of the $\log \tau_\alpha$ vs. T_g/T curve for systems with small ratios T_g/θ_D turns from convex (i.e., super-Arrhenius) to concave (i.e., sub-Arrhenius). In other words, in the case

of significant quantum effects the apparent activation energy (the slope of $\log \tau_\alpha$ *vs.* $1/T$) decreases upon approaching T_g, in contrast to the traditionally observed increasing. Thus, the analysis in the framework of the elastic model of the glass transition predicts that quantum effects will lead to an unusual temperature dependence of the structural relaxation time upon approaching T_g, that will result in a low fragility and might lead to an apparent fragile-to-strong crossover in the temperature dependence of $\tau_\alpha(T)$. We note that of course the Debye approximation for the temperature dependence of MSD in this model estimation does not present real fragile systems, where MSD increases non-linearly above T_g. However, even this approximation can illustrate a new qualitative feature that arises in the T-dependence of the structural relaxation time due to quantum effects, a kind of fragile–to–strong crossover.

A similar qualitative result can be obtained in the potential energy landscape approach. Let us consider the double-well potential picture of structural relaxation (fig. 2). When the over-barrier relaxation dominates, the activation energy of the structural relaxation is defined by the energy barrier height E_b. Upon cooling, the probability of tunneling from some level E_n will be higher than the probability of the over-barrier relaxation. As a result, $\tau_\alpha(T)$ will exhibit an apparent Arrhenius-like behavior with the activation energy E lower than E_b. A further decrease in T will lead to a higher probability of tunneling from the lower levels in the well, *i.e.* the apparent activation energy will decrease upon cooling. This will lead to a sub-Arrhenius temperature dependence and unusually low fragility. The latter can be as low as $m \sim 0$ if the tunneling from the zero-point level dominates the structural relaxation.

The presented in this section analysis shows that quantum effects should lead to unusual temperature variations of the structural relaxation. The rate of these variations (the slope of $\log \tau_\alpha$ *vs.* $1/T$) should decrease upon approaching T_g, while it only increases in most glass-formers. In other words, while all usual glass-forming liquids show only convex (super-Arrhenius) behavior of $\log \tau_\alpha$ *vs.* $1/T$, quantum effects might lead to a crossover from convex-to-concave (sub-Arrhenius) behavior of $\log \tau_\alpha$ upon approaching T_g. As a result, the glass transition range becomes significantly broader, the ratio T_g/T_m decreases significantly, and fragility might be unusually low. Indeed, low-T_g liquids exhibit rather low values of T_g/T_m (fig. 4) and fragility (fig. 5).

As we discussed in sect. 2, only light molecules are expected to have significant quantum effects in their structural dynamics. Among them, methane, ammonia and water are the most promising materials (fig. 1). However, only the dynamics of water have been studied in details, and below we will discuss the recently published studies on the dynamics of water close to T_g [25,36].

4 Quantum effects in bulk water

The zero-point energy of a H-bonded water network (O-H vibrations) is $\sim 2000\,\mathrm{K}$ [12], *i.e.* it is much higher
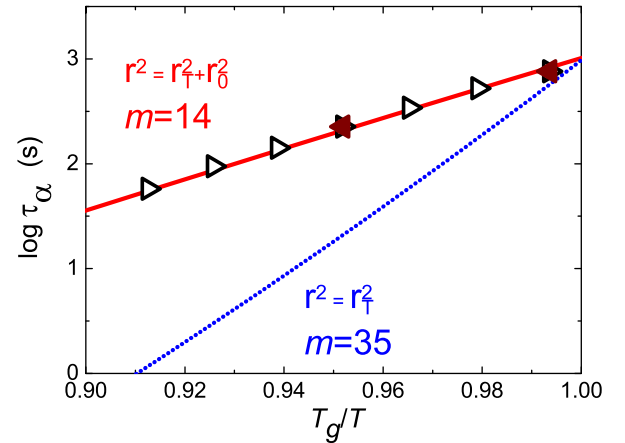

Fig. 7. Temperature dependence of τ_α in water close to T_g, and its estimates using total MSD (solid line), and MSD with neglected zero-point vibrations (dotted line) (data from [25]).

than the ambient temperature. Thus, large quantum effects in dynamics are expected. Yet most of the simulations completely disregard quantum effects in water. However, some of the simulations of water attempted to take quantum effects into account, *e.g.*, [12–14,45–48]. They demonstrated that even at ambient T, quantum effects lead to an increase of diffusion coefficients and a decrease of relaxation times by ~ 15–50%. Such quantum effects should be more pronounced at lower temperatures. Indeed, significant quantum effects in proton momentum distribution in supercooled water were found in simulations [47] and in a deep inelastic neutron scattering experiment [49]. These effects lead, in particular, to the excess of the mean kinetic energy of protons [49]. Tunneling of hydrogen was observed in various systems, including tunneling of atomic hydrogen in metals [50], and rotational tunneling of methyl CH_4 and ammonia NH_3 groups [6,51]. Recently, rotational tunneling of single water molecules confined in 5A beryl pores was also detected by inelastic neutron scattering [52]. There are signatures of the proton tunneling contributions to the structural relaxation spectra of ices [48,53–56].

Unfortunately, experimental studies of bulk water at low temperatures are prevented by crystallization. So, studies of bulk water dynamics at temperatures close to T_g are usually done either on low-density amorphous (LDA) water, prepared by a compression of ice at low T and the following annealing at $T \sim 130$–$140\,\mathrm{K}$, or on vapor-deposited (VD) samples [57–66]. Recent dielectric studies of VD and LDA water revealed [25,36,67] unusually low fragility, $m = 14$ (fig. 7), which is much lower than $m \sim 20$ known for the least fragile systems like SiO_2. Moreover, apparent Arrhenius dependence of $\tau_\alpha(T)$ results in unusually long $\tau_0 \sim 10^{-11}$–$10^{-10}\,\mathrm{s}$ (fig. 7). These studies also discovered an anomalously large isotope effect in T_g of bulk water, $\sim 12\,\mathrm{K}$ increase of T_g with H/D substitution [36] (fig. 8). This is significantly larger than the usual increase of less than $1\,\mathrm{K}$ observed in other hydrogen-bonding liquids [68,69]. All these unusual/anomalous dy-
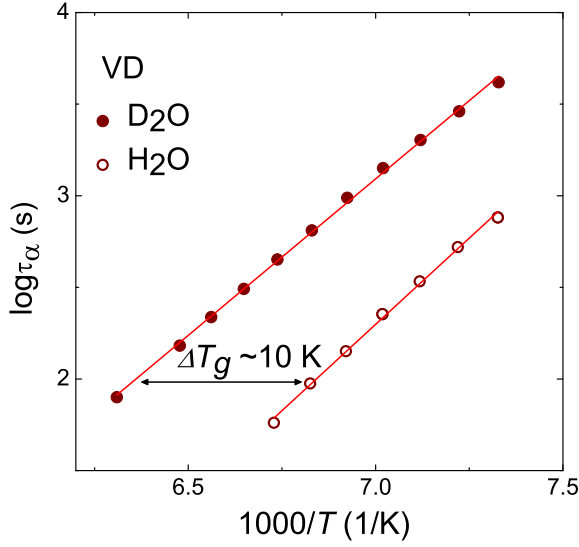
Fig. 8. Change of relaxation time and shift of T_g in deeply supercooled water due to the isotope effect [36]. Arrhenius fits are shown by solid lines (the fitting parameters are presented in table 1).
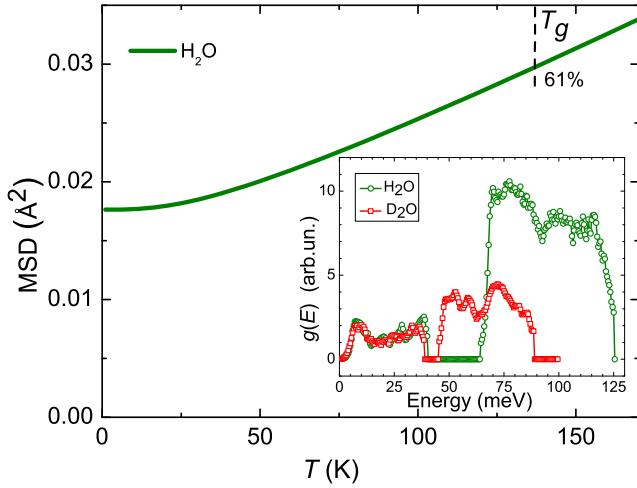

Fig. 9. MSD in LDA water (solid line) calculated using the vibrational density of states (inset). The dashed line marks the expected $T_g \sim 136\,\mathrm{K}$ of water. The inset shows the generalized vibrational density of states $g(E)$ for intermolecular vibrations in LDA water, H_2O (green symbols) and D_2O (red symbols), obtained from INS spectra [70–72].

namic properties of water can be well explained by quantum effects in structural relaxation [25,36].

The analysis of the vibrational density of states obtained using neutron scattering spectra revealed that r_0^2 contributes $\sim 60\%$ of the total MSD at T_g in water [25] (fig. 9). Thus indeed quantum effects are not negligible in water at temperatures close to T_g. This is also consistent with its relatively high Debye temperature $\theta_D \sim 2T_g$ [22]. It was shown in [25] that the elastic theory of glass transition (eq. (19)) with experimental MSD describes well the anomalously slow temperature variations of $\tau_\alpha(T)$ in supercooled water (fig. 7). It is a surprising result taking into account a good agreement of eq. (19) predictions

with the experimental data without any adjustable parameters (fig. 7). Moreover, disregarding the zero-point contribution to MSD of water in eq. (19) leads to a drastical contradiction with the experimental data. Thus, these results suggest that the contribution of quantum fluctuations to MSD indeed should be included into the elastic theory of glass transition. This analysis has been done in harmonic approximation. Anharmonic conributions to MSD in LDA ice are $\sim 6\%$ at $123\,\mathrm{K}$, and might reach 7% at $140\,\mathrm{K}$ [73]. The anharmonic contribution to the fragility (using eqs. (19) and (34)) is then of the order of $2\Delta r^2(T_g)/r^2(T_g) < 0.15$, where $\Delta r^2(T_g)$ is the anharmonic contribution to MSD. The difference of fragility with and without account for zero-point vibrations in water is about 250%, thus it is far larger than possible anharmonic corrections.

This low-temperature behavior of water does not match the well-studied high-temperature ($T > 235\,\mathrm{K}$) regime that corresponds to the super-Arrhenius (fragile) behavior [25] (fig. 10). This well-known puzzle has been noted already in ref. [74], and suggests an apparent fragile-to-strong crossover in water dynamics around 210–235 K [58,75–80]. Many researchers relate this anomaly to an underlying liquid-liquid phase transition in water in the temperature range $T \sim 210$–235 K [58,75–80]. Even results of computer simulations have been intensively discussed with regard to the existence of two phases of supercooled water [79,81]. A detailed analysis of the simulations of the ST2 water model [79] revealed a coexistence of two metastable liquid states with different densities. However, it is not obvious how well the ST2 model reproduces the real bulk water. Recent experimental studies using ultrafast X-ray diffraction revealed no phase transition in bulk water down to $T \sim 227\,\mathrm{K}$ [82]. Instead, the authors
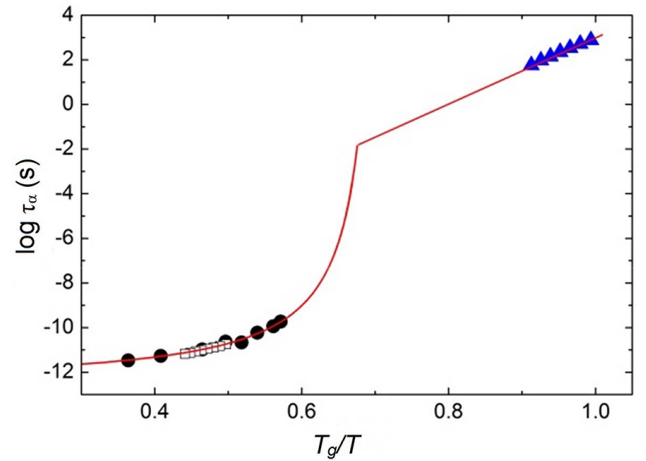
Fig. 10. Comparison of low-temperature (solid blue triangles) and high-temperature data for the structural relaxation time in water. Open squares: dielectric spectroscopy data in water [83]; solid black circles: shifted viscosity data [74]. The red line presents a schematic picture of the apparent fragile-to-strong crossover between high-temperature and low-temperature regimes. It was ascribed to a crossover from over-barrier relaxation to tunneling in [25,36].
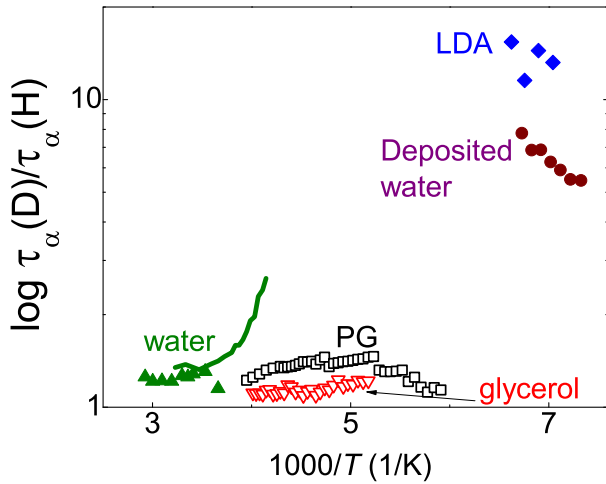
Fig. 11. The ratio of relaxation times in deuterated and protonated molecules, $\tau_\alpha(D)/\tau_\alpha(H) \sim 1.1$–1.3 for bulk water at $T > T_m$ (closed triangles), for glycerol (open squares) and propylene glycol (open triangles) in the entire T range. This ratio increases in supercooled water (solid line), and reaches $\tau_\alpha(D)/\tau_\alpha(H) \sim 10$ for LDA and deposited water (diamonds) at $T \sim 140$–136 K. Data are from [36] and references therein.

observed a smooth variation in the diffraction peaks reflecting a smooth improving of the tetrahedral structure upon cooling [82,84]. Recently, it was proposed [25,36] that the apparent fragile-to-strong crossover can reflect a crossover from the classical over-barrier relaxation to tunneling upon cooling bulk water (fig. 10). This behavior is consistent with the theoretical predictions discussed in sect. 3 (fig. 6).

Also the observed anomalously large isotope effect in the structural relaxation and T_g of water (fig. 8) is consistent with the tunneling process. In classical over-barrier relaxation, the change in the particles mass should only influence the characteristic prefactor τ_0 (assuming that structure and potential energy landscape are not affected by H/D substitution). In that case $\tau_0 \propto M^{1/2}$ should change between 5% and 40%, depending on the translational and rotational type of motions. Indeed, the isotope effect on water dynamics at high T is on the level $\sim$ 15–30% (fig. 11). The same weak isotope effect is observed in other H-bonding systems (glycerol and propylene glycol) in the entire temperature range where the relaxation times changes by more than 10 orders (fig. 11) [68,69]. However, in the case of supercooled water the isotope effect in dynamics increases sharply upon cooling, reaching $\sim 160\%$ at $T \sim 240$ K (fig. 11) [85]. Then, it exceeds 1000% at $T \sim 140$ K in LDA water [36]. So a strong (more than 10 fold) slowing-down in dynamics upon H/D substitution cannot be explained in the classical case. At the same time, tunneling probability depends exponentially on the mass of the particle and can increase significantly depending on the barrier's parameters (eq. (4)).

To describe the rate of structural relaxation in water, a model that takes into account the tunneling (sect. 2.1) was used in ref. [25]. There are 3 parameters defining the potential $U(x)$ (fig. 2): i) the curvature at the bottom

of the well, ii) the barrier height E_b, and iii) the barrier width at the bottom a (fig. 2). Here x is a configurational coordinate along the transition pass. To determine the parameters of the well we need a restriction imposed by the experimentally measured relaxation rates: The relaxation time should be $\sim 10^3$ s at $T = 136$ K, the apparent activation energy should be ~ 36 kJ/mol in the vicinity of T_g and τ_0 should correspond to the curvature of the potential at the bottom.

Dielectric spectroscopy measures the reorientation of dipole moments that can be connected to the rotation of H-atom(s) around the oxygen atom in water. In that case we can take the mass M in eq. (17) as a proton mass. This is also in agreement with the recent result of ref. [86] that molecular reorientation dynamics govern the glass transitions of the amorphous ices. The vibrational frequency in the well we can take ascribe to the librational mode. According to the vibrational spectrum of water (fig. 9) the librational mode is dominated by the peak in the range $\hbar\omega = 70$–120 meV. This energy fixes the value of $\tau_0 \sim 10^{-14}$ s and the curvature of the harmonic potential $U(x)$.

Using eq. (17) and the formulated-above restrictions, we obtained $E_b - E_0 = 46 \pm 1$ kJ/mol, rather independent of the choice of the librational frequency ω. The choice of the librational energy, however, affects strongly the distance of the tunneling: It was obtained that $a = 2.2 \pm 0.02$ Å for $\hbar\omega = 90$ meV, and $a = 1.9 \pm 0.02$ Å for $\hbar\omega = 120$ meV. Taking into account the simplicity of the model, these values of a are in a reasonable agreement with the jump length 1.5–1.9 Å found in supercooled water by the quasi-elastic neutron scattering [87] and NMR [85]. The estimated activation energy ~ 46 kJ/mol is comparable to that found by dielectric spectroscopy in different ices, 44–57 kJ/mol [54,88–92].

A 10-fold increase of the α-relaxation time in D_2O in comparison with H_2O can be explained also by a simple estimate. In H_2O apparent $\tau_0 \sim 10^{-11}$ s is by about 3 orders longer than the expected one based on the vibrational frequency, $\tau_0 \sim 10^{-14}$ s. This 3 orders difference is caused by the tunneling amplitude A_{tun}. In D_2O A_{tun} will be larger roughly by a square root of the D and H atoms mass ratio (eq. (4)), $(M_D/M_H)^{1/2} \sim 1.4$, *i.e.* the isotope effect increases the tunneling exponent A_{tun} by additional ~ 1.2 orders. This explains the factor of ~ 10 difference between τ_α in H_2O and D_2O. Also, according to the apparent Arrhenius fit (fig. 8), τ_0 in D_2O is actually by ~ 2 orders slower than in H_2O (table 1), which is still consistent with this rough estimate.

In spite of a very simplistic and schematic character of our estimate, it shows that the rotational tunneling effects can indeed lead to the experimentally measured fragility, $m = 14$, with the model parameters corresponding to the experimental values found in supercooled water. More accurate estimates are required to verify the probability of tunneling in realistic water potentials at low temperatures.

5 Quantum effects in confined water

Although water is one of the best materials for studying quantum effects in a supercooled liquid state, there is a
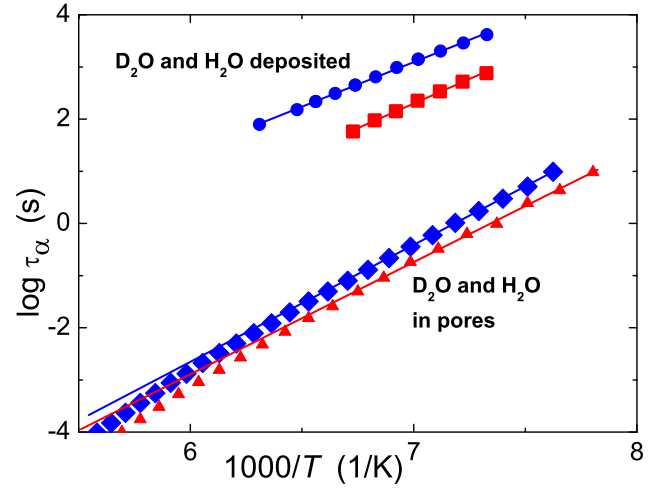
Table 1. Glass transition temperature T_g, fragility m, apparent activation energy E close to T_g and the respective pre-exponential factor τ_0.

	T_g (K)	m	E (kJ/mol)	$\log \tau_0$ (s)
Confined H_2O [95]	115	19.5 ± 1	41 ± 1	-15.7 ± 0.3
Confined D_2O [95]	118	19 ± 1	43 ± 1	-16.1 ± 0.1
Bulk VD H_2O [36]	136	14 ± 1	36 ± 1	-10.9 ± 0.3
Bulk VD D_2O [36]	146	13 ± 1	33 ± 1	-8.8 ± 0.3
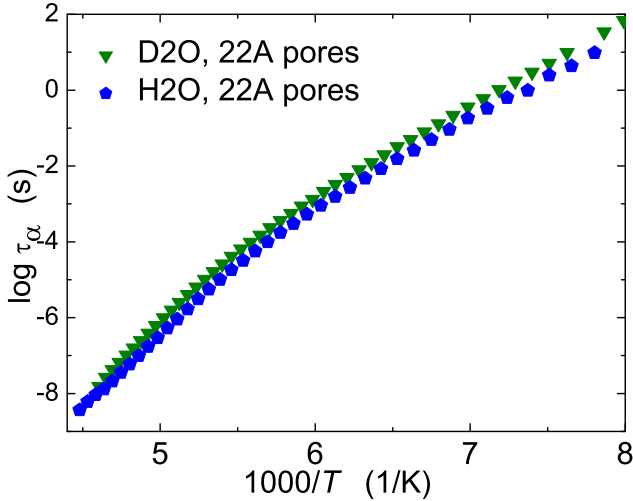
Fig. 12. Temperature dependence of the relaxation time estimated from the dielectric loss spectra of confined H_2O and D_2O [93].

Fig. 13. Low-temperature behavior of the dielectric relaxation time for vapor-deposited H_2O (red solid squares), vapor-deposited D_2O (blue solid circles) [36], confined H_2O (red triangles) and confined D_2O (blue diamonds) [95]. Solid lines present the Arrhenius fit of the low-temperature part of relaxation times. A comparison shows that deposited water has unreasonable values for τ_0 and fragility for classical over-barrier relaxation, while the data for confined water look reasonable.

major experimental problem —the fast crystallization of bulk water in the temperature range 230–160 K (the so-called "no man's land") that prevents studies of equilibrium bulk liquid water. To suppress crystallization, water can be studied in a strong confinement in the pores with diameter $\sim 2\,$nm or smaller. Quantum effects in hydrogen motion of strongly confined water are well known and are essential even at room temperature [52,93,94]. Coherent delocalization of protons in water in carbon nanotubes and the respective anomaly of momentum distribution has been measured using deep inelastic neutron scattering [94] at temperatures as high as 230 K. Recently, a new "quantum tunneling state" of water molecules confined in 5 Å channels in the mineral beryl was found using inelastic neutron scattering and computer simulations [52]. The authors have shown that the protons are delocalized and water molecules tunnel between six symmetrically equivalent positions in the beryl structure [52].

The influence of quantum effects on the dynamics of confined to 2.2 nm pores water was recently investigated in ref. [95]. These studies were able to cover a broad temperature range and indeed revealed an apparent fragile-to-strong crossover at $T \sim 180\,$K (fig. 12). However, this behavior is not specific for confined water and has been observed in many other strongly confined liquids (*e.g.*, ethylene glycol [96], salol [97], glycerol [98] and other confined liquids [99–101]). The glass transition temperatures

of confined water was found to be $\sim 115\,$K for H_2O and $\sim 118\,$K for D_2O, significantly lower than in the bulk water ($T_g \sim 136\,$K and 146 K, respectively [25,36]). The observed isotope shift of T_g, $\Delta T_g \sim 3\,$K is much smaller than that in the bulk water where $\Delta T_g \sim 10\,$K (fig. 8) [36], although it is large relative to other H-bonded liquids. All these results suggest a reduced role of the quantum effects in the structural dynamics of confined water.

The fragility of confined H_2O and D_2O is equal to ~ 19 (table 1) [95]. Although this value is extremely low, it is larger than the fragility of the bulk water ($m \sim 14$), again indicating smaller quantum effects in confined water. The low-temperature Arrhenius regime of confined and bulk water (fig. 12) have different activation energies. The apparent activation energy of the confined water $E \sim 41\,$kJ/mol is higher than that observed in the bulk LDA and VD water, $E \sim 36\,$kJ/mol [25]. The apparent Arrhenius behavior in confined water has a reasonable τ_0 for a light molecule, $\sim 10^{-15}$–$10^{-16}\,$s, in contrast to an unusually long $\tau_0 \sim 10^{-10}$–$10^{-11}\,$s observed in the bulk water [25] (fig. 13). Reasonable values of τ_0 and fragility (table 1) suggest no evidence of tunneling in strongly confined water, in contrast to the behavior of bulk VD and LDA water described above [25]. We note that, although the apparent activation energy in confined water appears to be significantly higher than in the bulk (41 kJ/mol *vs.* 36 kJ/mol), yet its relaxation time is $\sim 10^3$–10^4 times faster than in the bulk in the same temperature range (fig. 13).

Although tunneling does not give a significant contribution to the structural relaxation rate in 2.2 nm confined water, the quantum effects remain not negligible. A detailed analysis of the data (fig. 12 and table 1) reveals that the activation energy of the Arrhenius depen-
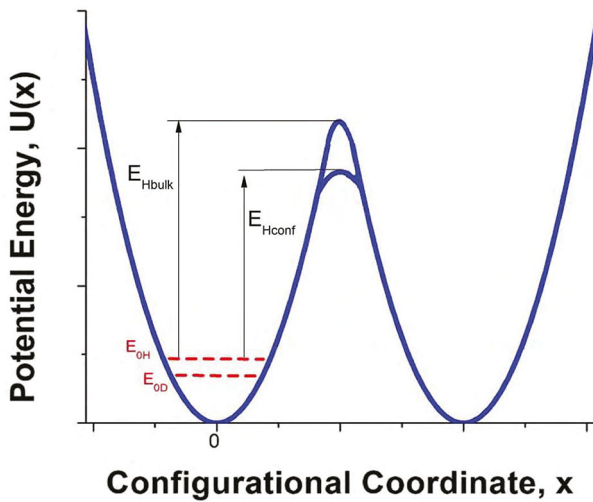
Fig. 14. Schematic presentation of a possible scenario for relaxation in bulk and confined water. The reduction of the energy barrier due to confinement leads to a higher probability of the over-barrier jumps than tunneling. However, the role of zero-point quantum fluctuations remains significant even in confined water, leading to a rather strong isotope effect.

dence is slightly ($\sim$ 1–2 kJ/mol) higher in confined D_2O than in confined H_2O (table 1). This difference most probably comes from the so-called trivial quantum effect, *i.e.*, a decrease of the activation energy due to zero-point energy $E_0 = \hbar\omega/2$ (fig. 14). As was discussed above, E_0 might be related to the energy of the librational mode of water molecules. It is $\hbar\omega \sim$ 70–90 meV for H_2O and it shifts to $\hbar\omega \sim$ 50–65 meV in D_2O (inset in fig. 9) [70–72]. This shift is consistent with the expected shift $\sim (M_D/M_H)^{1/2} \sim 1.4$, and corresponds to the change in the zero-point energy upon D/H substitution $\Delta(\hbar\omega/2) \sim$ 10–12 meV $\sim$ 1 kJ/mol. This value agrees well with the experimentally observed difference in the apparent activation energy of confined H_2O and D_2O at low temperatures (fig. 12, table 1), and suggests that the change in the zero-point energy is the major reason for the observed difference in the dynamics of confined H_2O and D_2O and their relatively strong shift of T_g.

The reason for the much smaller quantum effects in the dynamics of confined water in 2.2 nm pores can be related to the decrease of the energy barrier for structural relaxation upon confinement. As we discussed in sect. 5, the energy barrier for the relaxation observed in bulk LDA and VD at T close to T_g is $\sim$ 46 kJ/mol [25]. With this high-energy barrier, the probability for a proton (as a part of the rotation motion) to tunnel is higher than the probability to jump over the energy barrier at $T <$ 140–150 K [25, 36]. In confined water the activation energy for this relaxation is reduced $\sim$ 41 kJ/mol (fig. 14). Such reduction of the barrier height in strong confinement is known also for other liquids [68,69,96–98]. As a result, an over-barrier relaxation becomes more probable than tunneling in confined water. This leads to the normal value of the apparent τ_0 and significantly lower T_g in confined water (fig. 13). However, as we mentioned above, the smaller value of the

zero-point energy for librational motions in D_2O leads to a measurable change in the apparent activation energy upon D/H substitution, *i.e.* a slowing-down of the relaxation, and a relatively large shift in T_g between confined H_2O and D_2O. All these results emphasize a significant difference in the dynamics of bulk and confined water, and the important role the quantum effects play in water dynamics at low temperatures.

6 Summary and outlook

In this article we reviewed some possible nuclear quantum effects in the structural relaxation of supercooled liquids and their glass transition. Various criteria show that the quantum effects may be important for the structural dynamics of light molecular liquids only. The probability of quantum tunneling decreases exponentially with the mass of the moving particles suggesting that only lightest atoms/molecules might have significant quantum effects at not very low temperatures. These quantum effects should lead to several phenomena in the structural dynamics of liquids:

– extended supercooled range, *i.e.* unusually low ratio T_g/T_m;
– anomalously slow temperature variations of the structural relaxation close to T_g, *i.e.* very low fragility;
– sub-Arrhenius behavior of $\tau_\alpha(T)$, *i.e.* a decrease in the apparent activation energy of structural relaxation upon cooling;
– apparent fragile-to-strong crossover;
– anomalously large isotope effects.

As we discussed in the text, all these phenomena are observed in the dynamics of bulk water. These experimental data clearly suggest that the rotation of water molecule in the bulk might be dominating by tunneling even at temperatures $T \sim$ 130–150 K [25,36]. This is an unusually high temperature for tunneling in structural relaxation. It is caused by specifics of water molecule rotation —it involves only the motion of protons. According to the de Boer parameter (fig. 1), similar effects should be observed in liquids of other light molecules such as methane CH_4 and ammonia NH_3, and maybe also in liquid ethylene, ethane, oxygen and nitrogen. Indeed, rotational tunneling is known for the plastic phase of methane [6]. It would be interesting to study these liquids in a supercooled state where quantum effects including tunneling might dominate the dynamics.

Even if the tunneling probability remains lower than the over-barrier relaxation, the zero-point energy can still play an important role in dynamics by effectively reducing the energy barrier, and by the sizeable contribution of zero-point quantum oscillations to the total mean squared atomic displacements. This should lead to the unusually low fragility of some low-T_g molecular liquids [96]. The importance of the zero-point energy has been emphasized in studies of confined water [95] and in the proton conductivity of phosphoric acids [102].

We emphasize that the presented theoretical picture is strongly simplified and does not take into account many important aspects. One of the important unsolved tasks is to take into account the indistinguishability of the particles and respective quantum statistics. Every particle is either a boson or a fermion. At low temperatures, in quantum regime, identical particles are indistinguishable, and the wave function of the system should be symmetrical for bosons and asymmetrical for fermions with respect to the permutation of any two particles. At non-zero temperature there is a coherence length that limits the size of the region where quantum indistinguishability is important. At larger distances decoherence due to thermal fluctuations makes the quantum correlations insignificant. The importance of quantum correlations for the structural dynamics was stressed recently on the example of liquid ^{4}He [103]. It was shown by simulations that the Bose statistics is the main factor that keeps ^{4}He in a liquid state all the way down to $T = 0$ under the pressure of its own vapor [103]. The Lindemann-like argument of high zero-point MSD in liquid ^{4}He is not sufficient to keep it liquid at low enough T [103]. One of the attempts to take into account quantum coherence was made in ref. [104]. It was based on the hypothesis that there are quantum correlations in water between each H^+ and the protons of the surrounding water molecules, leading to the formation of coherent dissipative structures. This approach predicted that an anomalous decrease of H^+ conductance in H_2O-D_2O mixtures would take place [105], and it was confirmed experimentally [106]. Later evidence of quantum correlation effects of protons and deuterons in water was found by the analysis of the Raman spectra of liquid H_2O-D_2O [107]. However, no study of the possible effect of quantum correlations on the structural relaxation in water or other light molecule systems is known, although some simulation work was promised to be done in future [11].

Our last comment is related to simulations of water. It is known that despite many existing potentials, none of them can consistently describe the structure, dynamics and other properties of water in a broad enough temperature range. Based on the presented-here discussion we suggest that disregarding quantum effects might be one of the major problem in simulations of water. The zero-point energy even for librational motions is $\sim 500\,\mathrm{K}$, *i.e.* much higher than ambient T. Neglecting it in simulations is usually compensated by the deformation of the potential energy landscape and results in an inadequate description of the hydrogen bonding in water. We suspect that simulations of water molecules will be successful only when quantum effects will be explicitly taken into account. These effects are indeed negligible for most of other molecules because their zero-point energy is usually much smaller than T_g or ambient temperature, and then any quantum corrections might be small. But this is not the case for water, methane and ammonia, and maybe for some other light molecular liquids.

Author contribution statement

Both authors contributed equally to this paper.

References

1. R.C. Zeller, R.O. Pohl, Phys. Rev. B **4**, 2029 (1971).
2. P.W. Anderson, B.I. Halperin, C.M. Varma, Philos. Mag. **25**, 1 (1972).
3. P. Esquinazi (Editor), *Tunneling Systems in Amorphous and Crystalline Solids* (Springer, 1998).
4. W.A. Phillips (Editor), *Amorphous Solids: Low-Temperature Properties* (Springer, Berlin, 1981).
5. W.A. Phillips, Rep. Prog. Phys. **50**, 1657 (1987).
6. W. Press, *Single Particle Rotations in Molecular Crystals*, Springer Tracts Mod. Phys., Vol. **92** (Springer, Berlin, 1981).
7. V.A. Benderskii, D.E. Makarov, C.A. Wight, *Chemical Dynamics at Low Temperatures* (John Wiley & Sons, Inc., NY, 1994).
8. C. Chakravarty, J. Chem. Phys. **103**, 10663 (1995).
9. T.E. Markland, J.A. Morrone, B.J. Berne *et al.*, Nat. Phys. **7**, 134 (2011).
10. C. Chakravarty, J. Phys. Chem. A **115**, 7028 (2011).
11. T.E. Markland, J.A. Morrone, K. Miyazaki, B.J. Berne, D.R. Reichman, E. Rabani, J. Chem. Phys. **136**, 074511 (2012).
12. L. Wang, M. Ceriotti, T.E. Markland, J. Chem. Phys. **141**, 104502 (2014).
13. S. Habershon, T.E. Markland, D.E. Manolopoulos, J. Chem. Phys. **131**, 024501 (2009).
14. T.F. Miller III, D.E. Manolopoulos, J. Chem. Phys. **123**, 154504 (2005).
15. L. Proville, D. Rodney, M.-C. Marinica, Nat. Mater. **11**, 845 (2012).
16. J. de Boer, in *Progress in Low Temperature Physics*, edited by J.C. Gorter, Vol. **2** (North-Holland, Amsterdam, 1957).
17. C. Chakravarty, J. Chem. Phys. **103**, 10663 (1995).
18. L.D. Landau, L.M. Lifshitz, *Quantum Mechanics* (Butterworth-Heinemann, Oxford, 1981).
19. D. Waxman, A.J. Leggett, Phys. Rev. B **32**, 4450 (1985).
20. F.A. Lindemann, Physik. Z. **11**, 609 (1910).
21. D. Turnbull, Contemp. Phys. **10**, 473 (1969).
22. V.N. Novikov, A.P. Sokolov, Phys. Rev. Lett. **110**, 065701 (2013).
23. J.C. Dyre, N.B. Olsen, T. Christensen, Phys. Rev. B **53**, 2171 (1996).
24. J.C. Dyre, Rev. Mod. Phys. **78**, 953 (2006).
25. A.L. Agapov, A.I. Kolesnikov, V.N. Novikov, R. Richert, A.P. Sokolov, Phys. Rev. E **91**, 022312 (2015).
26. R.W. Hall, P.G. Wolynes, J. Chem. Phys. **86**, 2943 (1987).
27. U. Buchenau, R. Zorn, Europhys. Lett. **18**, 523 (1992).
28. V.N. Novikov, A.P. Sokolov, Phys. Rev. E **67**, 031507 (2003).
29. C.M. Roland, K.L. Ngai, J. Chem. Phys. **104**, 2967 (1996).
30. F.W. Starr, S. Sastry, J.F. Douglas, S.C. Glotzer, Phys. Rev. Lett. **89**, 125501 (2002).
31. L. Larini, A. Ottochian, C. De Michele, D. Leporini, Nat. Phys. **4**, 42 (2008).

32. D.S. Simmons, M.T. Cicerone, Q. Zhong, M. Tyagi, J.F. Douglas, Soft Matter **8**, 11455 (2012).
33. B.A. Pazmiño Betancourt, P.Z. Hanakata, F.W. Starr, J.F. Douglas, Proc. Natl. Acad. Sci. U.S.A. **112**, 2966 (2015).
34. A.A. Maradudin, E.W. Montroll, G.H. Weiss, *Theory of Lattice Dynamics in the Harmonic Approximation* (Academic Press, New York, 1963) Chapt. VII.
35. V.N. Novikov, E.A. Rössler, Polymer **54**, 6987 (2013).
36. C. Gainaru, A.L. Agapov, V. Fuentes-Landete, K. Amann-Winkel, H. Nelson, K. Köster, A.I. Kolesnikov, V.N. Novikov, R. Richert, R. Böhmer, T. Loerting, A.P. Sokolov, Proc. Natl. Acad. Sci. U.S.A. **111**, 17402 (2014).
37. F. Mallamace, C. Branca, C. Corsaro, N. Leone, J. Spooren, S.-H. Chen, H.E. Stanley, Proc. Natl. Acad. Sci. U.S.A. **107**, 22457 (2010).
38. C.A. Angell, J. Non-Cryst. Solids **73**, 1 (1985).
39. C.A. Angell, Science **267**, 1924 (1995).
40. R. Böhmer, K.L. Ngai, A.C. Angell, D.J. Plazek, J. Chem. Phys. **99**, 4201 (1993).
41. Q. Qin, G.B. McKenna, J. Non-Cryst. Solids **352**, 2977 (2006).
42. A. Agapov, V.N. Novikov, A. Kisliuk, R. Richert, A.P. Sokolov, J. Chem. Phys. **145**, 234507 (2016).
43. W. Huang, S. Shahriari, R. Richert, J. Chem. Phys. **123**, 164504 (2005).
44. S. Shahriari, A. Mandanici, L.M. Wang, R. Richert, J. Chem. Phys. **121**, 8960 (2004).
45. M. Ceriotti, J. Cuny, M. Parrinello, D.E. Manolopoulos, Proc. Natl. Acad. Sci. U.S.A. **110**, 15591 (2013).
46. B. Chen, I. Ivanov, M.L. Klein, M. Parrinello, Phys. Rev. Lett. **91**, 215503 (2003).
47. J.A. Morrone, R. Car, Phys. Rev. Lett. **101**, 017801 (2008).
48. B. Pamuk, J.M. Soler, R. Ramirez, C.P. Herrero, P.W. Stephens, P.B. Allen, M.-V. Fernandez-Serra, Phys. Rev. Lett. **108**, 193003 (2012).
49. A. Pietropaolo, R. Senesi, C. Andreani, A. Botti, M.A. Ricci, F. Bruni, Phys. Rev. Lett. **100**, 127802 (2008).
50. H. Wipf, A. Magerl, S.M. Shapiro, S.K. Satija, W. Thomlinson, Phys. Rev. Lett. **46**, 947 (1981).
51. M. Prager, A. Heidemann, Chem. Rev. **97**, 2933 (1997).
52. A.I. Kolesnikov, G.F. Reiter, N. Choudhury, T.R. Prisk, E. Mamontov, A. Podlesnyak, G. Ehlers, A.G. Seel, D.J. Wesolowski, L.M. Anovitz, Phys. Rev. Lett. **116**, 167802 (2016).
53. M.-S. Chen, L. Onsager, J. Bonner, J. Nagle, J. Chem. Phys. **60**, 405 (1974).
54. F. Bruni, G. Consolini, G. Careri, J. Chem. Phys. **99**, 538 (1993).
55. S.F. Fisher, G.L. Hofacker, in *Physics of Ice*, edited by N. Riehl, B. Bullemer, H. Engelhardt (Plenum, New York, 1969).
56. M. Benoit, D. Marx, M. Parrinello, Nature **392**, 258 (1998).
57. R.S. Smith, B.D. Kay, Nature **398**, 788 (1999).
58. C.A. Angell, Chem. Rev. **102**, 2627 (2002).
59. G.P. Johari, J. Chem. Phys. **122**, 144508 (2005).
60. A. Hallbrucker, E. Mayer, G.P. Johari, J. Phys. Chem. **93**, 4986 (1989).
61. G.P. Johari, A. Hallbrucker, E. Mayer, Nature **330**, 552 (1987).
62. G.P. Johari, A. Hallbrucker, E. Mayer, Science **273**, 90 (1996).
63. D.R. MacFarlane, C.A. Angell, J. Phys. Chem. **88**, 759 (1984).
64. Y.P. Handa, D.D. Klug, J. Phys. Chem. **92**, 3323 (1988).
65. C.A. Tulk, D.D. Klug, R. Branderhorst, P. Sharpe, J.A. Ripmeester, J. Chem. Phys. **109**, 8478 (1998).
66. M.S. Elsaesser, K. Winkel, E. Mayer, T. Loerting, Phys. Chem. Chem. Phys. **12**, 708 (2010).
67. K. Amann-Winkel, C. Gainaru, P.H. Handle, M. Seidl, H. Nelson, R. Böhmer, T. Loerting, Proc. Natl. Acad. Sci. U.S.A. **110**, 17720 (2013).
68. L.P. Singh, R. Richert, Rev. Sci. Instrum. **83**, 033903 (2012).
69. M.A. Ramos, C. Talón, R.J. Jiménez-Riobóo, S. Vieira, J. Phys.: Condens. Matter **15**, S1007 (2003).
70. A.I. Kolesnikov, J.C. Li, S. Dong, I.F. Bailey, R.S. Eccleston, W. Hahn, S.F. Parker, Phys. Rev. Lett. **79**, 1869 (1997).
71. J. Li, A.I. Kolesnikov, J. Mol. Liq. **100**, 1 (2002).
72. J. Li, J. Chem. Phys. **105**, 6733 (1996).
73. D.D. Klug, E. Whalley, E.C. Svensson, J.H. Root, V.F. Sears, Phys. Rev. B **44**, 841 (1991).
74. C.A. Angell, J. Phys. Chem. **97**, 6339 (1993).
75. K. Ito, C.T. Moynihan, C.A. Angell, Nature **398**, 492 (1999).
76. P.H. Poole, F. Sciortino, U. Essmann, H.E. Stanley, Nature **360**, 324 (1992).
77. S.-H. Chen, L. Liu, E. Fratini, P. Baglioni, A. Faraone, E. Mamontov, Proc. Natl. Acad. Sci. U.S.A. **103**, 9012 (2006).
78. C.A. Angell, Science **319**, 582 (2008).
79. J.C. Palmer, F. Martelli, Y. Liu, R. Car, A.Z. Panagiotopoulos, P.G. Debenedetti, Nature **510**, 385 (2014).
80. P. Gallo, K. Amann-Winkel, C.A. Angell *et al.*, Chem. Rev. **116**, 7463 (2016).
81. D.T. Limmer, D. Chandler, J. Chem. Phys. **135**, 134503 (2011).
82. J.A. Sellberg, C. Huang, T.A. McQueen *et al.*, Nature **510**, 381 (2014).
83. R. Buchner, J. Barthel, J. Stauber, Chem. Phys. Lett. **306**, 57 (1999).
84. A.K. Soper, Nat. Mater. **13**, 671 (2014).
85. J. Qvist, C. Mattea, E.P Sunde, B. Halle, J. Chem. Phys. **136**, 204505 (2012).
86. J.J. Shephard, C.G. Salzmann, J. Phys. Chem. Lett. **7**, 2281 (2016).
87. J. Qvist, H. Schober, B. Halle, J. Chem. Phys. **134**, 144508 (2011).
88. O. Yamamuro, M. Oguni, T. Matsuo, H. Suga, J. Phys. Chem. Solids **48**, 935 (1987).
89. S.R. Gough, D.W. Davidson, J. Chem. Phys. **52**, 5442 (1970).
90. H. Suga, S. Seki, Faraday Discuss. Chem. Soc. **69**, 221 (1980).
91. G.P. Johari, E. Whalley, J. Chem. Phys. **115**, 3274 (2001).
92. O. Wörz, R.H. Cole, J. Chem Phys. **51**, 1546 (1969).

93. G.F. Reiter, A.I. Kolesnikov, S.J. Paddison, P.M. Platz-man, A.P. Moravsky, M.A. Adams, J. Mayers, Phys. Rev. B **85**, 045403 (2012).

94. G. Reiter, C. Burnham, D. Homouz *et al.*, Phys. Rev. Lett. **97**, 247801 (2006).

95. A. Agapov, V.N. Novikov, A. Kisliuk, R. Richert, A.P. Sokolov, J. Chem. Phys. **145**, 234507 (2016).

96. H.E. Stamley (Editor), *Liquid Polymorphysm*, Adv. Chem. Phys., Vol. **152** (Wiley, Hoboken NJ, 2013).

97. M. Arndt, R. Stannarius, H. Groothues, E. Hempel, F. Kremer, Phys. Rev. Lett. **79**, 2077 (1997).

98. M. Arndt, R. Stannarius, W. Gorbatschow, F. Kremer, Phys. Rev. E **54**, 5377 (1996).

99. F. Kremer (Editor), *Dynamics in Geometrical Confine-ment* (Springer, New York, 2014).

100. R. Richert, Annu. Rev. Phys. Chem. **62**, 65 (2011).

101. M. Alcoutlabi, G.B. McKenna, J. Phys.: Condens. Matter **17**, R461 (2005).

102. M. Heres, Y. Wang, P.J. Griffin, C. Gainaru, A.P. Sokolov, Phys. Rev. Lett. **117**, 156001 (2016).

103. M. Boninsegni, L. Pollet, N. Prokof'ev, B. Svistunov, Phys. Rev. Lett. **109**, 025302 (2012).

104. C.A. Chatzidimitriou-Dreismann, E. Brandas, Int. J. Quantum Chem. **37**, 155 (1990).

105. C.A. Chatzidimitriou-Dreismann, Int. J. Quantum Chem. Symp. **23**, 153 (1989).

106. H. Weingartner, C.A. Chatzidimitriou-Dreismann, Nature **346**, 548 (1990).

107. C.A. Chatzidimitriou-Dreismann, U.K. Krieger, A. Möller, M. Stern, Phys. Rev. Lett. **75**, 3008 (1995).

Vladimir Novikov received his B.S. in Physics from the Novosibirsk State University and a PhD from the Institute of Nuclear Physics of the Russian Academy of Sciences. He then worked at the Academy of Sciences on the vibrational and relaxational dynamics of disordered materials. In 2010 he joined the research faculty of the Chemistry Department at the University of Tennessee. His current research focuses on the dynamics of glasses and supercooled liquids, including polymers.

Alexei Sokolov received a PhD in Physics in 1986 from the Russian Academy of Sciences. He worked several years in Germany before joining the faculty at the University of Akron, USA, in 1998. In 2009 he accepted the Governor's Chair position at the University of Tennessee and Oak Ridge National Laboratory, where he currently leads the Soft Matter group. He is a Fellow of the American Physical Society and of the AAAS. His current research interest focuses primarily on the dynamics of soft materials, including topics of the glass transition, polymer and biomolecular dynamics, composite materials and materials for energy applications.